

Dynamic Voltage Stability Analysis for Power Systems with Wind Power Plants using Relative Gain Array (RGA)

Li-Jun Cai*, István Erlich**, Jens Fortmann***

*REpower Systems SE, Albert-Betz-Strasse 1, D-24783 Osterroenfeld, Germany. (e-mail: lijun.cai@repower.de)

**Institute of Electrical Power Systems - University of Duisburg-Essen 47057, Germany. (e-mail: erlich@uni-duisburg.de)

***REpower Systems SE, Albert-Betz-Strasse 1, D-24783 Osterroenfeld, Germany, (e-mail: jens.fortmann@repower.de)

Abstract: This paper concerns the use of relative gain array (RGA) for analyzing the interactions among the wind power plant voltage controller and power system traditional voltage stability controllers. RGA analyses for both static and dynamic voltage stability controls are carried out based on the multi-input multi-output (MIMO) transfer function matrix $\mathbf{J}_v(s)$. By means of the singular value and RGA, the dynamic voltage stability and their controller interactions are analyzed and the dynamic voltage stability control loop selection can be realized. A multi-machine power system with a wind power plant is simulated for the demonstration of the proposed approach. The proposed approach takes the advantages of the classical static voltage stability analysis and the modern multi-variable feedback control theory. This proposed approach is simple and can be easily implemented into large power systems with distributed wind power plant voltage controllers.

Keywords: Doubly-fed induction generator, wind turbine voltage control, wind power plant voltage control, dynamic voltage stability, singular value analysis, relative gain array

1. INTRODUCTION

Many large modern wind power plants apply doubly-fed induction generators (DFIGs). These machines are collectively referred to as variable speed machines and they possess important advantages such as reactive power control capabilities, smaller and cheaper converter compared with a full size one. Furthermore, the voltage control of the DFIG wind turbine could reinforce the system voltage and dynamic stability (Rueda, J.L. and Shewarega, F. (2009)).

Because of the increasingly integration of such large wind power plants, their impacts on power system static and dynamic behavior must be analyzed. Also, their interaction with conventional power plants and power system control must be taken into consideration.

This paper provides a method to analyze the influence of wind power plant voltage control and other power system controllers on the power system dynamic voltage stability by means of the relative gain array (RGA).

Similar to the method introduced in (Cai, L.J. and Erlich, I. (2005)), the bus voltage magnitudes are considered as outputs and all possible control variables as inputs of the multi-input and multi-output (MIMO) model. Then the MIMO transfer function matrix of the power system is analyzed by means of singular value decomposition (SVD). For selecting the proper feedback control signal and control loop which provides little interactions with the other control loops, the RGA method is employed. The controller interactions can be analyzed for all

critical frequencies and the most suitable control loops will be selected.

This paper is organized as follows: Following the introduction, wind turbine and wind power plant voltage control strategy will be introduced in Section 2. Then the RGA analysis for the dynamic voltage stability control is described in detail in Section 3. The simulation results of the RGA analyses are given in Section 4. Finally, brief conclusions are deduced.

2. VOLTAGE CONTROL SCHEME OF DFIG AND WIND POWER PLANT

2.1 Structure of DFIG

The basic example structure of DFIG is shown in Fig. 1. As a general approach, the space-phasor coordinates with orthogonal direct (d) and quadrature (q) axes are used. The choice of the stator voltage as the reference frame enables the decoupled control of P (active power, d control channel) and Q (reactive power, q control channel) (Cai, L.J. and Erlich, I. (2005), Bristol, E. H. (1966)).

2.2 Wind power plant layout and control signals

According to Grid Codes, active and reactive power should be controlled at the point of common coupling (PCC), which is usually located at medium or high voltage side of the wind power plant transformer. Therefore the wind power plant controller can be installed at the PCC, as shown in Fig. 2 (Bluhm, R. and Fortmann, J. (2010)).

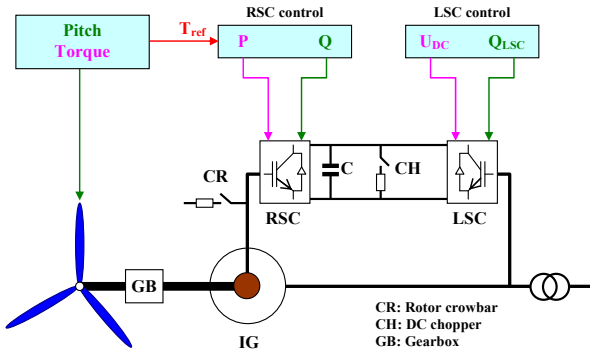


Fig. 1. Structure of DFIG

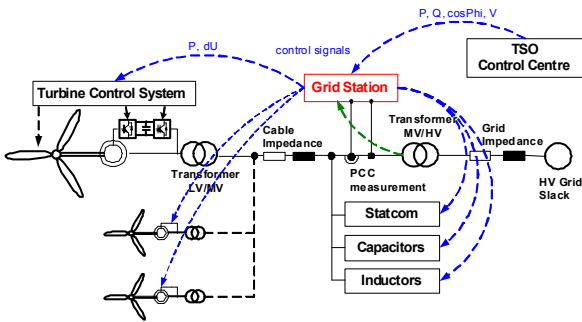


Fig. 2. Basic layout of wind power plant control

The wind power plant controller can receive active and reactive power setpoints from the Control Centre of the system operator. A classical control mode is a power factor setpoint at the PCC controlled by the wind power plant controller, which will send reactive power setpoints to all turbines. In case of voltage control, there is a voltage setpoint at the PCC.

This paper employs voltage control method at PCC in combination with local voltage control at the wind turbine level (Bluhm, R. and Fortmann, J. (2010)). Optionally, external reactive power compensation can be connected to the PCC and can be controlled by the wind power plant controller. This is only necessary, if the reactive power range of the wind turbine is not sufficient to fulfill the requirements at the PCC.

The basic function of a voltage controller is to calculate the setpoint for reactive power depending on the voltage. A general block diagram for a proportional characteristic is shown in Fig. 3. The voltage measurement (U_{meas}) is subtracted from the voltage setpoint (U_{set}) to calculate the voltage deviation (ΔU). This deviation is multiplied by the proportional control factor KVC to calculate the reactive power setpoint (Q_{set}). Depending on the desired control characteristic, a reactive current setpoint (I_{q_set}) can also be used (Bluhm, R. and Fortmann, J. (2010)).

The voltage control can be implemented in both turbine level (local) and the wind power plant level (central) and the detailed description can be found in (Bluhm, R. and

Fortmann, J. (2010)). A combination of the central and local voltage control can combine their favorable characteristics with benefit for grid stability. The continuous voltage control at the turbine level delivers a very fast response to deep voltage drops and also to small voltage deviations inside the standard operation range (Bluhm, R. and Fortmann, J. (2010)).

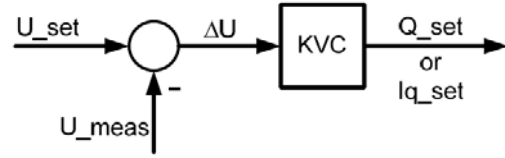


Fig. 3. Proportional voltage control block diagram.

The combination with voltage control at the wind power plant level ensures an exact adjustment of the required reactive power value at the grid connection point. A stable control of the combined controller can be guaranteed because the time constant of the subordinate local control is more than 10 times faster than the time constant of the wind power plant controller. Settings such as slope or response time of the combined voltage control can be easily adapted to achieve the desired characteristics required at different connection points or in different countries (Bluhm, R. and Fortmann, J. (2010)).

The above mentioned wind power plant voltage control characteristic will be applied for analyzing its influence on the power system voltage stability.

3. RGA ANALYSIS FOR VOLTAGE STABILITY CONTROL

The RGA was introduced as a steady state measure of interactions for multivariable, decentralized control (Bristol, E. H. (1966)). It was later extended to the frequency domain (Milanovic, J.V. and Duque, A.C.S. (2004), Skogestad, S. and Postlethwaite, I. (1996)). In MIMO control system, the RGA is mainly used to analyze the interactions among different controllers. It allows us to match up input-output variables that have the biggest effect on each other, without having undesirable effects on the others (Milanovic, J.V. and Duque, A.C.S. (2004)). The definition and properties of RGA will be introduced in this section.

3.1 Definition of RGA

For a multivariable system, the RGA is defined as the matrix of relative gains (Skogestad, S. and Postlethwaite, I. (1996)). If a multivariable system is defined by the matrix equation

$$\mathbf{y}(s) = \mathbf{J}_v(s) \cdot \mathbf{d}(s) \quad (1)$$

where

$\mathbf{J}_v(s)$ is the transfer function matrix for the dynamic voltage stability analysis defined in (Cai, L.J. and Erlich, I. (2005)).

$\mathbf{d}(s)$ and $\mathbf{y}(s)$ are vectors that contain the selected input and output variables.

The relative gain $\gamma_{ij}(s)$ for an input $d_j(s)$ and an output $y_i(s)$ is then defined by the ratio of the uncontrolled gain and the controlled gain, as shown in (2) (Milanovic, J.V. and Duque, A.C.S. (2004), Skogestad, S. and Postlethwaite, I. (1996)).

$$\gamma_{ij} = \frac{\text{Controlled gain between } y_i(s) \text{ and } d_j(s)}{\text{Uncontrolled gain between } y_i(s) \text{ and } d_j(s)}$$

$$= \frac{\left. \frac{y_i(s)}{d_j(s)} \right|_{d_k(s)=0, k \neq j}}{\left. \frac{y_i(s)}{d_j(s)} \right|_{y_k(s)=0, k \neq j}} \quad (2)$$

The uncontrolled gain is the gain between the input $d_j(s)$ and the output $y_i(s)$ when all other outputs are uncontrolled, as shown in Fig. 4. This gain is the element $g_{ij}(s)$ of multivariable transfer function matrix $\mathbf{J}_v(s)$ (Milanovic, J.V. and Duque, A.C.S. (2004), Skogestad, S. and Postlethwaite, I. (1996)).

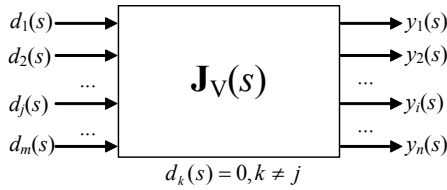


Fig. 4. Uncontrolled gain

The controlled gain is the gain between the input d_j and the output y_i when perfect control is exercised at the rest of the outputs (i.e., their value is zero), as given in Fig. 5 (Cai, L.J. and Erlich, I. (2005), Milanovic, J.V. and Duque, A.C.S. (2004), Skogestad, S. and Postlethwaite, I. (1996)).

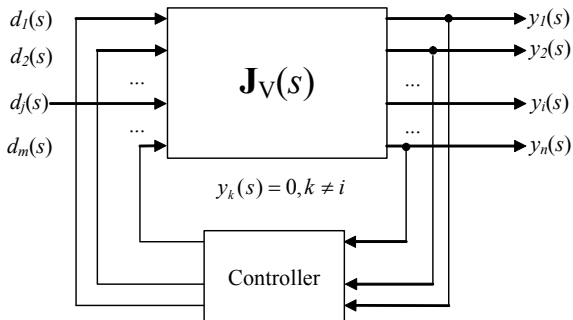


Fig. 5. Controlled gain

Hence, for the input $d_j(s)$ and the output $y_i(s)$, RGA element $\gamma_{ij}(s)$ measures the effect that the control of the rest of the variables has on gain between $y_i(s)$ and $d_j(s)$ (Milanovic, J.V. and Duque, A.C.S. (2004), Skogestad, S. and Postlethwaite, I. (1996)).

3.2 Calculation of RGA

A direct or uncontrolled gain of g_{ij} (between input $d_j(s)$ and output $y_i(s)$) is given by the elements of the multivariable transfer function $\mathbf{J}_v(s)$ (Milanovic, J.V. and Duque, A.C.S. (2004), Skogestad, S. and Postlethwaite, I. (1996)).

The controlled gain $\hat{g}_{ij}(s)$ of input $d_j(s)$ and output $y_i(s)$ is inverse of the j^{th} element $\mathbf{J}_v^{-1}(s)$ (Skogestad, S. and Postlethwaite, I. (1996)). In this paper, since the $\mathbf{J}_v(s)$ is a non-square transfer function matrix, $\mathbf{J}_v^{-1}(s)$ represents the pseudo-inverse of the $\mathbf{J}_v(s)$. Hence, the relative gain for input d_j and output y_i is (Skogestad, S. and Postlethwaite, I. (1996)):

$$\gamma_{ij}(s) = \frac{\Delta g_{ij}(s)}{\hat{g}_{ij}(s)} = [\mathbf{J}_v(s)]_{ij} \times [\mathbf{J}_v^{-1}(s)]_{ji} \quad (3)$$

And the matrix of all relative gains is:

$$\Gamma(s) = \mathbf{J}_v(s) \times [\mathbf{J}_v^{-1}(s)]^T \quad (4)$$

where \times is the element-by-element multiplication or Schur product (Bristol, E. H. (1966)).

RGA is calculated based on the multivariable frequency response. In frequency domain, it involves inversion of complex matrix whose size is determined by the number of the inputs and the outputs to the system (Milanovic, J.V. and Duque, A.C.S. (2004)).

3.2 Main properties of RGA

The main algebraic and control properties of the RGA are given in (Milanovic, J.V. and Duque, A.C.S. (2004), Skogestad, S. and Postlethwaite, I. (1996)). Only the most important control properties associated with the dynamic voltage stability control are selected in this section:

1. The RGA depends only on plant model and not on the controller. It is calculated for the open loop system.
2. It is independent on the input and the output scaling, i.e., it is not influenced by the choice of units.
3. The negative inverse of the RGA element is equal to the ratio of relative change in the element of $\mathbf{J}_v(s)$ and its transpose inverse:

$$\frac{d[\mathbf{J}_v^{-1}(s)]_{ji}}{[\mathbf{J}_v^{-1}(s)]_{ji}} = -\gamma_{ij}(s) \frac{dg_{ij}(s)}{g_{ij}(s)} \quad (5)$$

4. In case those RGA elements are large, the elements of the inverted matrix $\mathbf{J}_v^{-1}(s)$ are very sensitive to changes in the elements of $\mathbf{J}_v(s)$. Therefore, plants having large RGA elements are very sensitive to model uncertainty.

The most important property of the RGA for voltage stability analysis is that RGA is independent on scaling, it depends only on the plant model and not on the controller and that the RGA elements measure their own sensitivity to uncertainty.

3.3 Control loop pairing using RGA

As shown in the definition and the properties of RGA, it provides a measure of control loops interactions and gives an indication of control loop pairings. The interpreting of the results of RGA is given as follows:

$$\gamma_{ij}(s) = 1$$

Uncontrolled gain and controlled gain are identical and interaction does not affect the pairing of the input d_j and the output y_i .

$$\gamma_{ij}(s) = 0$$

Uncontrolled gain is zero, i.e. d_j has no effect on y_i .

$$0 < \gamma_{ij}(s) < 1$$

Other control loops interaction increases gain. The interaction is most severe when $\gamma_{ij}(s) = 0.5$.

$$1 < \gamma_{ij}(s) < 10$$

Other control loops interaction reduces gain. Higher controller gains are required.

$$\gamma_{ij}(s) \gg 10$$

The pairing of variables with large RGA elements is undesirable. It can indicate a system sensitive to small variations in gain and possible problems applying model based control techniques.

$$\gamma_{ij}(s) < 0$$

Controlled gain is in opposite direction from the uncontrolled gain.

Therefore, considering the above interpretations, the objective is to pair the input and output variables where $\gamma_{ij}(s)$ is nearest to 1 while avoiding the $\gamma_{ij}(s)$ which are zero or negative. Therefore, the following control input and output pairings should be avoided:

1. Small elements: a zero element means a lack of input and output relationship.
2. Negative elements: this implies a change of sign in gain between open and closed loop.
3. Very large elements: this means that closed loop sensitivity is much less than open loop and mean that there will be substantial interaction among the control loops.

4. SIMULATION RESULTS

A typical four-machine two-area power system model mentioned in (Cai, L.J. and Erlich, I. (2005)), as shown in Fig. 6, is used for demonstration of the proposed method. The synchronous generators are represented by 6th order model. The governors, static exciters, power system stabilizers (PSS) are also considered. Induction motor loads are modelled at Bus 4 (deep bar and leakage inductance saturation) and Bus 9 (double cage and leakage inductance saturation). For the

typical wind application, a wind power plant with 40MW is applied on Bus 11.

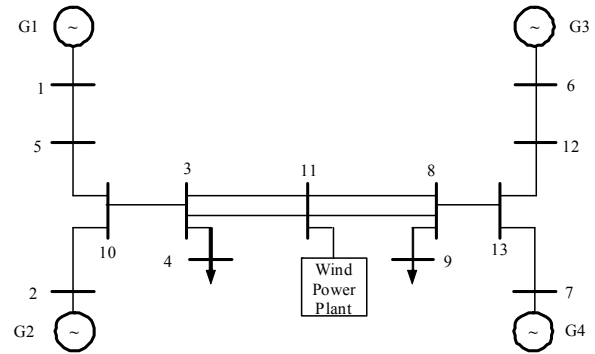


Fig. 6. Four machine two area power system

4.1 RGA analysis

Two different scenarios are simulated for the RGA analyses:

1. RGA analyses with different operating conditions.

In order to simulate the uncertainty of the wind power plant production, different operating conditions of the test system are simulated. The whole trend is that the wind power plant generation at Bus 11 is increasing for simulating the fluctuation of the wind power.

2. RGA analyses with different load modulations.

In order to analyze the increasing distributed generation in power system, reactive modulations are added to the other PQ buses 4 and 9. The RGA analyses are then carried out to find the most suitable control signal for the dynamic voltage stability behavior.

For the above mentioned two scenarios, the RGA for steady state ($s=0$) and inter-area mode oscillation frequencies are analyzed.

4.2 Steady state ($s=0$)

a) Steady state RGA with different operating conditions

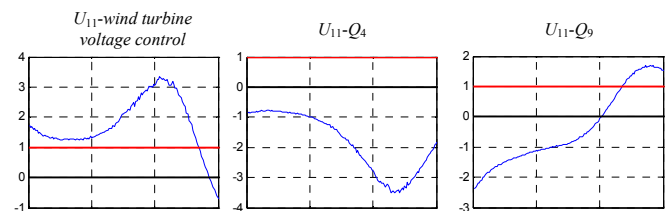


Fig. 7. Steady state RGA of Bus 11 voltage magnitude for different operating conditions

Steady state RGAs are analyzed with different operating conditions. Based on the singular value analysis mentioned in (Cai, L.J. and Erlich, I. (2005)), buses 3, 4, 8, 9 and 11 are the most critical ones associated with the steady state voltage

stability. Since the Bus 11 is the most critical one, it is selected to demonstrate the simulation result.

In this paper, only the inputs for critical nodes (11, 4 and 9) are illustrated, where X-axis represents different operating conditions with the increasing of the wind generation and Y-axis represents the RGA value.

From the simulation results given in Fig. 7, it is obvious that with the variation of operating point, the RGA will also be changed. Following conclusions can be derived:

1. With the variation of the operating point, only part of the operation points have RGA in the range of [0.5 3], (i.e. U_{11-Q9} and U_{11} -wind power voltage control in Fig. 7). The wind power plant voltage control is suitable for the steady state voltage stability control in this operating range.
2. In case that the RGAs outside the range of [0.5 3], the RGA can be used as a measure to remove the control signals which have the severe interactions with the other outputs.
3. For each new operating point, the RGA must be recalculated to select the proper control loop pairing for steady state voltage stability control.
4. The RGAs associated with the voltage controls (DFIG wind turbine and synchronous generator) vary always in a range of [0.5 3]. Furthermore, from different load modulation analyses, the input singular vectors associated with the wind turbine voltage control are relatively large (Cai, L.J. and Erlich, I. (2005)). Therefore, DFIG wind turbine voltage control is suitable for improving steady state voltage stability. Furthermore, it has also lower interactions with the other control loops.
5. The RGAs of U_{11-Q4} are too small and the reactive modulation at nodes 4 is not suitable for the steady state voltage stability control of U_{11} .

b) Steady state RGA with different load modulations

Focusing on one basic operating condition of the test system (Milanovic, J.V. and Duque, A.C.S. (2004), Skogestad, S. and Postlethwaite, I. (1996)), the numbers of load modulations are increased. In this paper, two load modulations at Bus 4 and Bus 9 are presented. Similar to the analysis performed in (Cai, L.J. and Erlich, I. (2005)), Bus 11 is selected to demonstrate the simulation result.

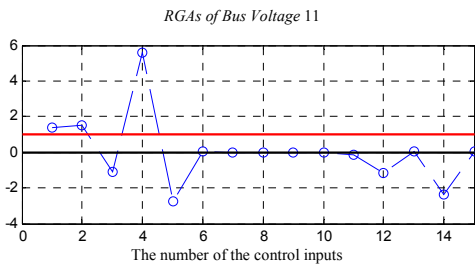


Fig. 8 Steady state RGA with different load modulations

The input numbers and their corresponding input variables are given in Table I and II.

From Fig. 8, it can be seen that the control number 1 (wind power plant voltage control signal) and control number 2 (the active power control of generator 1 (Bus 1)) are all with RGA close to 1. However, the generator active power control is not selected as the suitable control signal for the steady state voltage stability control, because:

1. Though the generator active power control has the least interaction with the other control loops, this active power control is not a suitable for the voltage control.
2. Furthermore, this control signal is not a local signal for the Bus 11 voltage control.

Therefore, the wind power plant voltage control signal is the possible local control signal for the Bus 11 voltage magnitude control in the steady state.

4.3 Inter-area mode

a) Inter-area mode RGA with different operating conditions

For the inter-area mode of oscillation frequency (Cai, L.J. and Erlich, I. (2005)), RGAs are analyzed with different operating conditions. Since the Bus 11 is the most critical one, it is selected to demonstrate the simulation result.

Similar to the steady state analysis, only the inputs for critical nodes (11, 4 and 9) are illustrated, where X-axis represents different operating conditions with the increasing of the wind generation and Y-axis represents the RGA value.

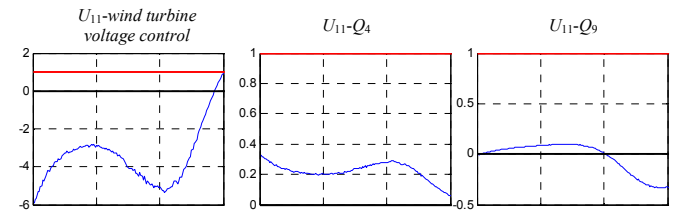


Fig. 9 RGA with different operating conditions for the inter-area mode of oscillation frequency

Since the RGAs associated with wind turbine voltage control, $Q4$ and $Q9$ are all quite small, they cannot be applied for the inter-area mode of dynamic voltage stability.

b) Inter-area mode RGA with different load modulations

Focusing on one basic operating condition, the numbers of load modulations are increased. Bus 11 is also selected to demonstrate the simulation result.

With the $Q4$ and $Q11$ increase of load modulations, the RGAs of some input and output pairs are tended to 1. This means that with the increase of load modulations, the voltage magnitude of each node may be controlled decentralized using the local or nearby feedback signal.

4.4 DFIG voltage control for system voltage stability

For the distributed generation, following conclusions could be deduced for their contribution to power system voltage stability:

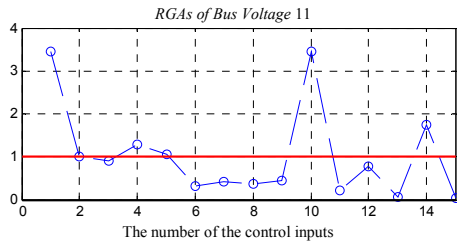


Fig. 10 RGA with different load modulations for the inter-area mode of oscillation frequency

1. Since the wind power plants are distributed in power system and their active power generation fluctuate, RGA will also be changed with their power generation. Therefore, for every new operating point, the RGA must be recalculated to select the proper control loop pairing for steady and dynamic voltage stability control.
2. Unlike the RGA analysis performed in (Milanovic, J.V. and Duque, A.C.S. (2004)), the input and output signals are selected for the dynamic voltage stability analysis. Therefore, the RGA plots in this research do not reveal the critical modes of oscillation frequencies. However, the critical modes of oscillation frequencies can be obtained from the maximal singular value plot, as described in (Cai, L.J. and Erlich, I. (2005)).
3. For the dynamic voltage stability controller design of wind power plant, method mentioned in Cai, L.J. (2004) could be applied.

5 CONCLUSION

This paper concerns the use of RGA for analyzing the interactions among the power system dynamic voltage stability control loops. RGA analyses for both static and dynamic voltage stability controls are carried out. A typical multi-machine power system with a wind power plant is simulated for the demonstration of the proposed approach. This approach takes the advantages of the classical static voltage stability analysis and the modern multi-variable feedback control theory. Since the input and output signal can be limited to a small range, this approach can be easily implemented into large power system with distributed generation.

REFERENCES

Bluhm, R. and Fortmann, J. (2010), Advanced two level voltage control in wind farms with doubly fed induction generators, presented at *EWECE 2010*.
 Bristol, E. H. (1966), On a new measure of interaction for multivariable process control, *IEEE Trans. Automat. Contr.*, vol. AC-11, pp. 133–134, Jan. 1966.
 Cai, L.J. (2004), *Robust coordinated control of FACTS devices in large power systems*, Logos Verlag, Berlin, ISBN: 3-8325-0570-9.

Cai, L.J. and Erlich, I. (2005), *Dynamic Voltage Stability Analysis in Multi-Machine Power Systems*, Published in *15th Power System Computation Conference 2005 Liege, Belgium*, August 22-26.
 Custsem, T.V. and Vournas (1998), C., *Voltage stability of the electric power systems*, Kluwer academic publishers, Boston/London/Dordrecht, ISBN 0-7923-8139-4.
 Hingorani, N.G. and Gyugyi, L. (2000), *Understanding FACTS – Concepts and technology of Flexible AC Transmission Systems*, IEEE Press, 2000. ISBN 0-7803-3455-8.
 Kundur, P. (1993), *Power system stability and control*, McGraw-Hill, Inc, ISBN 0-07-035958-X.
 Larsen, E.V. and Chow, J.H. (1987), SVC control design concepts for dystem dynamic performance, *Application of Static Var Systems for System Dynamic Performance, IEEE Publication 87th, 0187-5-PWR*, pp. 36–53.
 Milanovic, J.V. and Duque, A.C.S. (2004), Identification of Electromechanical Modes and Placement of PSSs Using Relative Gain Array, *IEEE Trans. Power Systems*, vol. 19, pp. 410-417, February 2004.
 Rogers, G. (1999), *Power System Oscillations*, Kluwer Academic Publishers, ISBN: 0-7923-7712-5.
 Rueda, J.L. and Shewarega, F. (2009), Small signal stability of power systems with large scale wind power integration, presented at the *XIII ERIAC Regional Iberoamericano DE CIGRE*.
 Skogestad, S. and Postlethwaite, I. (1996), *Multivariable feedback control – Analysis and design*, John Wiley & Sons, ISBN: 0-471-94330-4, July 1996.

APPENDICES

TABLE I

The Input Numbers and Their Corresponding Input Variables for the Wind Power Plant Voltage Control Signal and Generation Modulations

Input Number	1	2	3	4	5	6	7	8	9
	Wind Power Voltage Control	Active Generation Modulation				Reactive Generation Modulation			
Input Variable	<i>wind_sig</i>	P_1	P_2	P_6	P_7	Q_1	Q_2	Q_6	Q_7

TABLE II

The Input Numbers and Their Corresponding Input Variables for the Active and Reactive Load Modulations

Input Number	10	11	12	13	14	15	16	17	18	19
Input Variable	P_4	Q_4	P_9	Q_9	P_{11}	Q_{11}	P_3	Q_3	P_5	Q_5

Input Number	20	21	22	23	24	25	26	27
Input Variable	P_8	Q_8	P_{10}	Q_{10}	P_{12}	Q_{12}	P_{13}	Q_{13}